CO5-1　Production of technetium-99 by neutron irradiation of molybdenum trioxide

T. Kubota, T. Chida[1] and Y. Niibori[1]
Institute for Integrated Radiation and Nuclear Science, Kyoto University

[1]*Department of Quantum Science and Energy Engineering, Tohoku University*

INTRODUCTION: Technetium-99 is a pure beta emitter with a half-life of 2.11×10^5 (y) and is a fission product with its yield of 6.0%. Technetium forms anionic TcO_4^- to be mobile species under oxidic condition. Hence, its migration behavior in the environment is an important research field for the safety assessment on the disposal of high-level radioactive waste [1]. Investigations on the interaction of ^{99}Tc with various materials in the environment require methods other than radiation measurement, such as spectrophotometry, due to its weak radioactivity. In this report the production of adequate amount of ^{99}Tc tracer was investigated.

EXPERIMENTS: Technetium-99 was produced by the neutron irradiation of natural isotopic molybdenum. A 2 g of MoO_3 powder was encapsulated in a quartz test tube under vacuum and the test tube was placed in an aluminum capsule filled with water. The capsule was irradiated for 47 hours at the reactor power of 1 MW and then for 6 hours at 5 MW in the Hydraulic Conveyer Facility (Hyd.) of the Kyoto University Reactor (KUR). Technetium-99 was recovered by solvent extraction at 75 days after irradiation. The MoO_3 powder irradiated was dissolved with NaOH and then contacted with methyl ethyl ketone (MEK) [2]. The radioactivity of NaOH and MEK phase was measured by γ-spectrometry. The amount of ^{99}Tc produced was evaluated from the radioactivity of ^{99m}Tc by assuming that ^{99m}Tc was in radioactive equilibrium with ^{99}Mo at the end of irradiation.

RESULTS: The gamma ray spectrum of initial NaOH solution in the Fig. 1 shows no 145 keV gamma ray line of ^{99m}Tc on the contrary strong lines of ^{134}Cs and ^{124}Sb. The line of ^{99m}Tc is found in MEK solution after the solvent extraction, which yielded the distribution ratio of ^{134}Cs and ^{124}Sb was lower than 1/1000. Theses impurities would be completely removed by repeated solvent extraction. Besides ^{99m}Tc, in Fig. 1 shows the 155 keV line of ^{188}Re, which was determined by its half-life of 0.71 d in Fig. 2. It is reasonable that ^{188}Re was produced from tungsten as an impurity in MoO_3. Tungsten is a homologous element of molybdenum; thus, its amount is likely to be larger than other elements. The radioactivity of ^{99m}Tc finally decreased to lower than the detection limit, which shows no ^{99}Mo extracted in MEK phase and high separation efficiency of ^{99m}Tc and ^{99}Tc. The amount of ^{99}Tc was evaluated from that of ^{99}Mo at the end of irradiation to be 4.6 nmol, if ^{99}Mo and ^{99m}Tc is totally decayed. In conclusion, ^{99}Tc can be separated from Mo as a target material and antimony, cesium, and tungsten as an impurity by using solvent extraction with MEK and the irradiation of as much as 30 g MoO_3 would yield an enough amount for an optical analysis.
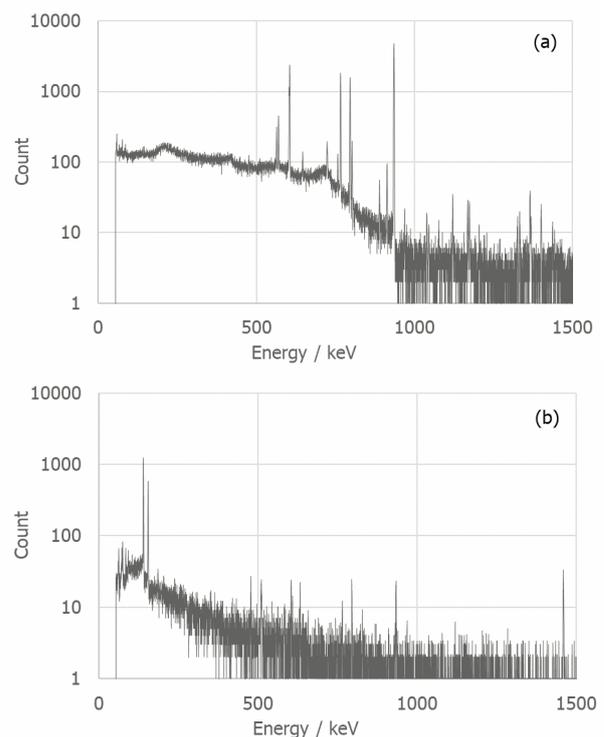

Fig. 1. Gamma ray spectra from high purity germanium detector. (a) NaOH solution. (b) MEK solution
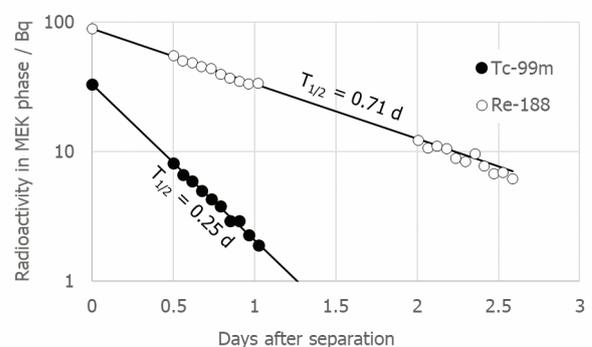

Fig. 2. Radioactive decay curve of ^{99m}Tc and ^{188}Re

REFERENCES:
[1] S. Luksic *et al.*, J. Nucl. Mat., **466** (2015) 526-538.
[2] P. Martini *et al.*, App. Rad. Iso., **139** (2018) 325-331

R2004

CO5-2   Volcanic and Tectonic History of Philippine Sea Plate (South of Japan) Revealed by ^{40}Ar/^{39}Ar Dating Technique

O. Ishizuka, S. Sekimoto[1], R. Okumura[1], H. Yoshinaga[1], Y. Iinuma[1], T. Fujii[2]

Geological Survey of Japan, AIST

[1]*Institute for Integrated Radiation and Nuclear Science, Kyoto University*

[2]*Graduate School of Engineering, Osaka University*

INTRODUCTION: Submarine volcanic rocks are known to give ages different from their true eruption ages in some cases. This is due to the existence of excess ^{40}Ar in the rapidly quenched glass or Ar loss and K remobilization caused by reaction with seawater or hydrothermal fluids. Stepwise-heating analysis in ^{40}Ar/^{39}Ar dating is particularly useful for dating submarine volcanics.

Tectonic reconstruction of the Philippine Sea Plate for the period immediately before and after subduction initiation at ~52 Ma to form the Izu-Bonin-Mariana (IBM) arc is prerequisite to understand cause of subduction initiation (SI) and test competing hypotheses for SI such as spontaneous or induced nucleation. There is increasing evidence that multiple geological events related to changing stress fields took place in and around Philippine Sea plate about the time of SI ~52 Ma (e.g., Ishizuka et al., 2020). It is important to understand the pattern and tempo of these geological events, particularly the duration and extent of seafloor spreading in the proto arc associated with SI, and its temporal relationship with spreading in the West Philippine Basin (WPB).

EXPERIMENTS: Samples were wrapped in an aluminum foil packet and the packets were piled up in a pure aluminum (99.5% Al) irradiation capsule (9 mm diameter and 30 mm long). The irradiation capsule was partitioned into 3 compartments to minimize the horizontal flux variation across the capsule, and was wrapped with Cd foil to suppress contribution of thermal neutron.

For the experiments described here, around 5 mg of sample was analysed. Only minimum acid leaching was applied to the glass samples, i.e., ultrasonic cleaning with 3M HCl for 10 minutes at room temperature. In case of altered samples, they were leached with HCl, and then HNO$_3$ at 95°C using hot stirrer. After this acid treatment, the samples were examined under binocular microscope before packed for irradiation.

RESULTS: Recent cruises (KS-17-15 and YK19-07S cruises) in the Philippine Sea basins investigated origin and age of formation of ocean basins in and around the Daito Ridge group. The data are still preliminary, but some fresh basalt samples returned well-defined ^{40}Ar/^{39}Ar ages older than the age of onset of subduction along the IBM arc at c. 52 Ma. Combined with interpretation of seafloor magnetic anomaly data, this strongly implies that some part of the Philippine Sea basins such as the West Philippine Basin existed prior to the IBM arc, and this basin could be a part of overriding plate at subduction initiation.

Temporal variation of geochemical characteristics of basalts in the Philippine Sea basins appears to indicate that major compositional variation occurred in sub-Philippine Sea mantle subsequent to subduction initiation. This might imply that sinking of large volume of Pacific Plate along the entire IBM arc margin triggered counterflow of asthenospheric mantle and reorganization of sub-Philippine Sea mantle.

The Kita-Daito Basin separates the Amami Plateau and the Daito Ridge, both of which belong to the Daito Ridge Group. No rock sampling has been reported from this basin to constrain its age and origin of this basin. The Vp model of the Kita-Daito Basin suggests the presence of a $4 - 6$ km thick crust, similar to the backarc basin oceanic crust in the Shikoku and Parece Vela Basins, as revealed by Nishizawa et al. (2011, 2013). These features seem to imply that rifting and seafloor spreading occurred between the Amami Plateau and Daito Ridge to form the Kita-Daito Basin. Dredge sampling and Shinkai 6500 submersible survey observed and recovered samples from the crustal sections exposed in the deepest part of the basin. Collected samples are mostly composed of volcanic rocks, porphyries and trace amount of sedimentary rock and conglomerate. The volcanic rocks are basalt to andesite clasts. These samples show geochemical characteristics implying influence of material released from subducting slab. This implies that these rocks are not part of ocean crust composed of MORB. These volcanic rocks gave ages of middle Eocene, which indicates that these volcanic rocks formed after the period of subduction initiation of Izu-Bonin-Mariana arc. These observations seem to imply that the Kita-Daito Basin did not exist at the subduction initiation, and formed by rifting in middle Eocene accompanied by basaltic to andesitic volcanism (Fig. 1).
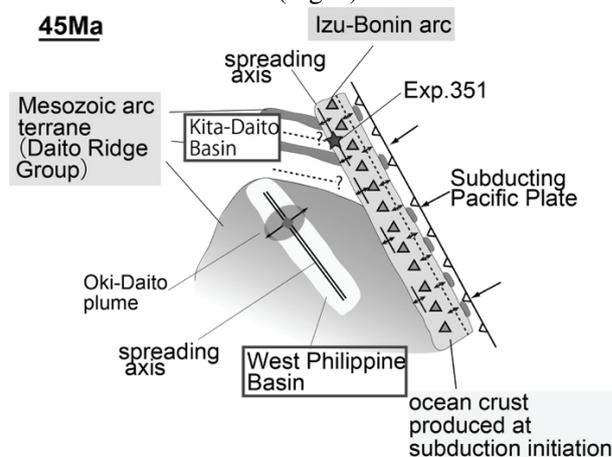

Fig. 1 Reconstruction of Philippine Sea Plate based on ArAr dating results.

CO5-3   Ar-Ar dating of basaltic rocks within accretionary complex to reconstruct the tectonic settings of paleo-Japanese archipelago

N. Hirano, H. Sumino[1], S. Sekimoto[2]

Center for Northeast Asian Studies, Tohoku University
[1] *Graduate School of Arts and Sciences, the University of Tokyo*
[2] *Institute for Integrated Radiation and Nuclear Science, Kyoto University*

INTRODUCTION:

Petit-spot submarine volcanoes erupted on an outer rise at the subducting NW Pacific Plate, recognized as new kind of volcano on the Earth [1]. Such volcanoes are likely ubiquitous in zones of plate flexure as several examples have been reported from oceanward slopes of trench in the world [2][3][4]. The widespread occurrence of petit-spot prior to plate subduction is supported by the reinterpretation of the origin of alkaline basalts found within accretionary complexes. The entrained xenolith from the depleted mantle is geochemically disturbed by the wall–rock interaction [5]. Tonegawa et al. [6] observed some structural changes in the NW Pacific crust and moho caused by the plate flexures and petit-spot volcanic activities. The accreted petit-spot would be a successful candidate to know the subsurface structure of subducting plates.

EXPERIMENTS:

We examined the "potential petit-spot" in Cretaceous accretionary complexes and forearc basins of the Pacific Rim (Chichibu Belts of SW Japan, Hidaka Belt of central Hokkaido, Tokoro and Nemuro Belts of E Hokkaido) (Fig. 1), and additionally with the Cretaceous seamounts on present western Pacific before their accretion.

Fig. 1. The sampling sites of basaltic rocks to analyze Ar-Ar datings in this study, shown by stars.

Radiometric Ar-Ar dating is commonly used to determine the ages of submarine lava samples, because the traditional K-Ar dating is impossible to remove the alteration part of fraction. The rock-samples, crushed to 100-500 μm grains, were irradiated by neutrons in the reactor, KUR, to produce ^{39}Ar from ^{39}K during three hours. During the irradiation, samples were packed with EB-1 biotite flux monitors, K_2SO_4 and CaF_2 as correcting factors in an aluminum capsule. The radiogenic ^{40}Ar, daughter nuclide of radioactive ^{40}K and parent, ^{39}Ar instead of ^{40}K, were simultaneously analyzed using a mass-spectrometer with an extraction technique of multi-step heating of approximately every 50 to 100 °C between 500 to 1500 °C at the University of Tokyo.
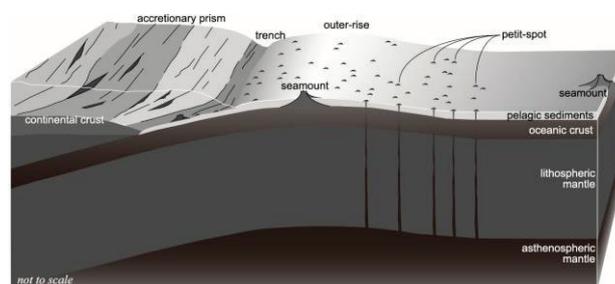

Fig. 2. Schematic model to accrete volcanic edifices on subducting plate.

RESULTS:

Although alkali basalts in the accretionary complex had traditionally been discriminated as ocean island basalts implying a seamount accretion, we newly report some of lavas, sills, and lamprophyres recognized as "accreted" petit-spots prior to plate subduction as well. They are all characterized by occurrences without reefal limestones [7]. Their Ar-Ar ages are generally younger than those of ocean island basalt because the petit-spot volcanisms occur at the outer-rise just prior to the plate-subduction (Fig. 2). In other way, we determined some seamounts and petit-spots on the present Pacific plate (around Minamitorishima Island) prior to its subduction as an analogue for the accreted basalts into accretionary complex. Their young and Paleogene Ar-Ar ages are first reported, implying the presence of petit-spot and post-Cretaceous volcanoes on present Western Pacific plate [8][9].

REFERENCES:
[1] N. Hirano et al., *Science*, **313** (2006), 1426-1428.
[2] N. Hirano et al., *Basin Res.*, **20** (2008), 543-553.
[3] N. Hirano et al., *Geochem. J.*, **47** (2013), 249-257.
[4] R. Taneja et al., *Gondwana Res.*, **28** (2014), 391-406.
[5] S. Pilet et al., *Nature Geosci.*, **9** (2016), 898-903.
[6] T. Tonegawa et al., *Earth Planets Space*, **70** (2018), 106.
[7] S. Sakai et al., *Geol. Mag.*, **158** (2021), 72-83.
[8] N. Hirano et al., *Deep-Sea Res. I*, **154** (2019), 103142.
[9] N. Hirano et al., *Island Arc*, **30** (2021), e12386.

CO5-4 INAA, Halogen Analysis, and Ar-Ar/I-Xe Dating for the Hayabusa2-return sample

R. Okazaki[1], S. Sekimoto[2], N. Iwata[3], N. Shirai[4], and Y. Miura[5]

[1]*Department of Earth and Planetary Sciences, Kyushu University*
[2]*KURNS*
[3]*Faculty of Science, Yamagata University*
[4]*Department of Chemistry, Tokyo Metropolitan University*
[5]*Earthquake Research Institute, University of Tokyo*

INTRODUCTION: In 2020 Dec, the spacecraft Hayabusa2 returned and brought back the samples collected from the asteroid Ryugu to the Earth [1, 2]. The Ryugu samples will be allocated to and studied by the initial analysis teams consisting of the 6 sub-teams, 1) chemistry (elements and isotopes), 2) petrology and mineralogy of coarse grains, 3) petrology and mineralogy of fine grains, 4) volatiles, 5) insoluble organic matter, and 6) soluble organic matter [3]. We belong to the volatile sub-team, and will conduct a combination analysis of INAA, halogen measurement, and Ar-Ar/I-Xe dating.

We have carried out rehearsal measurements since 2013 (project #: 25066, PI: S.S.), and established the analytical method.

The main object in this proposal is to evaluate the neutron flux variation among the samples irradiated, by using two orthoclase mineral standards that were located at the top and the bottom in one irradiation capsule. Gamma-ray measurements and noble gas analyses were also performed for various standard and meteorite samples as a realistic rehearsal for the Ryugu sample analysis.

EXPERIMENTS: Prepared samples for the November irradiation were three meteorite samples (Allende CV chondrite, Murchison CM chondrite, Bjurböle L/LL4 chondrite) and our standard samples (JB-1, BHVO-2, orthoclase, sanidine, and wollastonite). For the December irradiation, orthoclase, sanidine, and Allende samples were prepared. Each of the samples was placed in a conical dimple (φ1, depth ~ 0.5 mm) of a sapphire disk (φ5.5, 1.5 mm thick), and covered with a sapphire disk (φ5.5, 0.3 mm thick). Each of the sapphire container was wrapped with pure aluminum foil. These Al-wrapped containers were stacked and sealed in the capsules for the Long-term irradiation. Condition of the Long-term irradiations were 94 hours under 1MW-operation + 12 h under 5MW-operation and 141 hours under 1MW-operation + 18 h under 5MW-operation for the Nov and Dec irradiations, respectively.

In order to reduce the radioactivity from the sapphire containers and Al foil, the samples were moved to non-irradiated sapphire containers after the irradiation. Gamma-ray measurements of radioactive nuclides were performed at KURNS, preceding noble gas analysis at Kyushu Univ.

REUSLTS and DISCUSSION: The gamma-ray measurements for four Allende samples (the sample weights are 1.312 mg, 0.176 mg, 0.260 mg, and 0.162 mg) confirmed the homogeneity of the sample. Also, the homogeneity of JB-1 (1.090 mg, 0.681 mg, 0.966 mg) and BHVO-2 (1.037 mg, 1.094 mg, 0.827 mg) standard samples were confirmed.

Most of the ^{40}Ar concentrations in the orthoclase standard samples converges on the right value of 3.0E-4 cm^{3}STP/g, whereas a few data are away from the value (Fig. 1). This problem is due to the small sample size (~100 µg), and can be solved by multiple measurements. Comparing the average values, the December irradiation samples contain about 1.5 times more ^{39}Ar produced via the ^{39}K(n, p)^{39}Ar reaction than the November samples. The difference in the ^{39}Ar concentrations is in good agreement with that in the irradiation duration.

The concentrations of ^{39}Ar also depend on the location within the irradiation capsule. There is an about 20% difference between the two orthoclase samples irradiated in the Nov irradiation. These two samples were ca. 5cm apart each other, and other samples were between the two orthoclase samples. Therefore, the neutron flux should be corrected with respect to the sample location within the irradiation capsule.
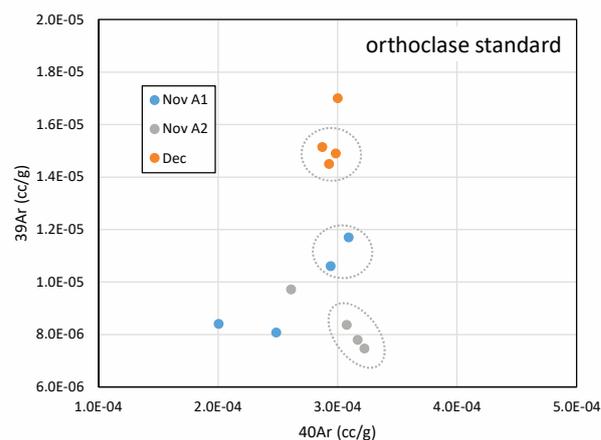

Fig. 1. Concentrations of ^{39}Ar and ^{40}Ar in the irradiated orthoclase standard samples

REFERENCES:
[1] Tachibana *et al.* 52nd Lunar and Planetary Science Conference, abstract #1289 (2021).
[2] Yada *et al.* 52nd Lunar and Planetary Science Conference, abstract #2008 (2021).
[3] Tachibana *et al.* American Geophysical Union, Fall Meeting 2018, abstract #P33C-3846 (2018).

R2030

CO5-5   Determination of Abundance of Rare Metal Elements in Seafloor Hydrothermal Ore Deposits by INAA Techniques-7: Cross check with ICP-QMS analysis

J. Ishibashi, Y. Sekiya[1], K. Yonezu[1], T. Nozaki[2], Y. Takaya[3], R. Okumura[4], Y. Iinuma[4] and K. Takamiya[4]

Department of Earth and Planetary Sciences, Faculty of Science, Kyushu University
[1]*Department of Earth Resources Engineering, Faculty of Engineering, Kyushu University*
[2]*Submarine Resources Research Center, Research Institute for Marine Resources Utilization, Japan Agency for Marine-Earth Science and Technology (JAMSTEC)*
[3]*Department of Systems Innovation, School of Engineering, the University of Tokyo*
[4]*Institute for Integrated Radiation and Nuclear Science, Kyoto University*

INTRODUCTION: Instrumental neutron activation analysis (INAA) has several advantages for geochemical tools to provide useful information for mineral exploration. For example, INAA enables highly sensitive multi-element analysis without geochemical pretreatment. We have conducted preliminary studies using mineralized samples collected from active seafloor hydrothermal fields, with a view to confirm and extend the range of application of this technique. Here, we report a result of cross check with inductively coupled plasma quadrupole mass spectrometry (ICP-QMS analysis).

EXPERIMENTS: Sulfide deposits collected from an active seafloor hydrothermal field in the Okinawa Trough were provided for a cross check analysis. For INAA analysis, 10-20 mg of powdered samples were irradiated at Pn-2 (thermal neutron flux = 5.5×10^{12} n/cm²/sec at 1 MW operation) for 25 minutes, and the gamma ray activity was measured for 15 minutes after adequate cooling time (~30 hours). ICP-QMS analysis followed procedure reported in other studies (Nozaki et al., 2021). Powdered samples weighing ca. 50 mg were dissolved by HNO_3-$HClO_4$-HF digestion in Teflon PFA screw-cap beakers, then heated overnight on a hot plate at 110 °C. The digested samples were progressively evaporated at 110 °C for more than 12 h, 130 °C for 3 h and 160 °C until dryness. The residue was dissolved in 5 mL Milli-Q de-ionized water combined with 4 mL HNO_3 and 1 mL HCl, then further diluted to 1:100 by mass (total dilution factor ca. 20,000) before introduction into the ICP-QMS (Agilent 7500ce).

RESULTS: A result of cross check is illustrated in Fig. 1, where content of eight elements (Au, Sb, Ag, As, Zn, Cu, Mn and Na) determined by INAA is plotted against that by ICP-QMS analysis, and plots are represented by element symbols. Basically, contents determined two analytical techniques well agreed, which supports analytical accuracy for trace element analysis employing INAA. A few plots are in the region beneath the diagonal line, which means notable discrepancies that content determined by INAA is lower than that by ICP-QMS. Such discrepancies are likely to be attributed to high background in the gamma ray spectrum due to excess activations of some specific nuclides.
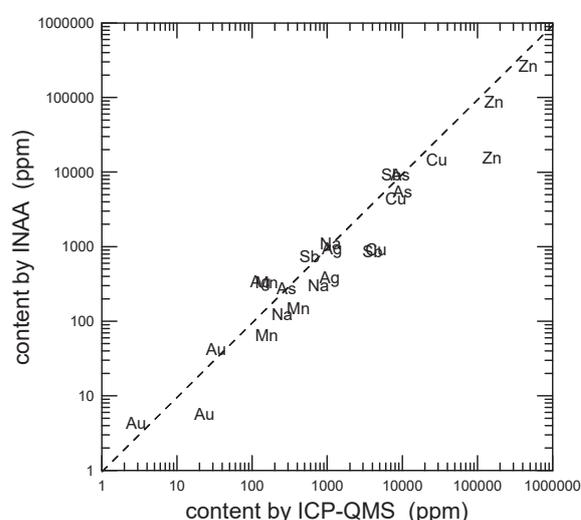

Fig. 1. A result of cross check analyses between ICP-QMS and INAA for three sulfide deposit samples. Contents of element (Au, Sb, Ag, As, Zn, Cu, Mn and Na) in each sample are plotted using element symbols.

[1] Nozaki *et al.*, Sci. Rep., **11**, 8809 (2021).

CO5-6 Size distribution of main constituents(Al,Ca,Fe) in soil particles of the atmospheric aerosols.

Norio Ito, Akira Mizohata, Yuto Iimura[1], Hisao Yoshinaga[1] Radiation Research Center, Osaka Prefecture University,[1] Institute for Integrated Radiation and Nuclear Science, Kyoto University

The soil particles in the atmosphere are main part of the coarse atmospheric aerosols in some land areas. At our observation site,Sakai,Osaka where a city and industry area can be found and about 2000 west from the China land , soil particles are locally produced from the near land surfaces such as raw earth surface, road surface and farmland and have the sources at the long distance areas, mainly coming from the China land, called Kosa mainly coming on spring. There might be the difference of element constituents in the locally produced soil particles and soil particles coming from China land. The difference could be the indicator of the contribution of the effect of the China land soil on the local soil effect. From the result of elemental constituent in coarse aerosol by the size distribution(small soil particle can come into

Sakai on the long distance) and seasonal change(on spring Kosa frequently comes) , we can investigate the effect of China land soil effect .

In this report,we analyze the size distribution of main constituents of soil particle, Al,Ca,Fe, of which concentrations are 1～10% using the Ca,Fe ratio to Al. The data is the analysis results of the elemental concentrations in the atmospheric aerosols observed at Sakai from 1995,about 50 sampling periods. In the sampling period(1 week) , the aerosols were collected by Andersen sampler that can separate the particles by 9 particle diameter range. The concentrations of element were obtained by the neutron activation analysis using Kyoto university neutron reactor.

From some results(period:2000-2003) of size distribution of Al,Ca,Fe(Fig.1), the soil particles can be found mainly coarse particle range (d>1.0μm) and on spring have higher concentrations than that of the other seasons. The ratios Ca/Al(Fig2a) show a flat behaviour on the particle size larger than 3μm, on smaller than 3μm the ratio decreasing. On the seasonally change of the ratio(Ca/Al), spring ratio, strongly effected from China land,has the smallest values suggesting the ratio(Ca/Al) is smaller than that of locally produced soil particles. On the other hand, the ratio (Fe/Al) has increase behaviour as the diameter decrease. This behaviour shows an different effect of the concentration difference of the China land soil particles. But the spring ratio(Fe/Ca) has the smallest values, indicating the source of Fe in the small particle(<2μm) might be particles from industry rather than soil particles.
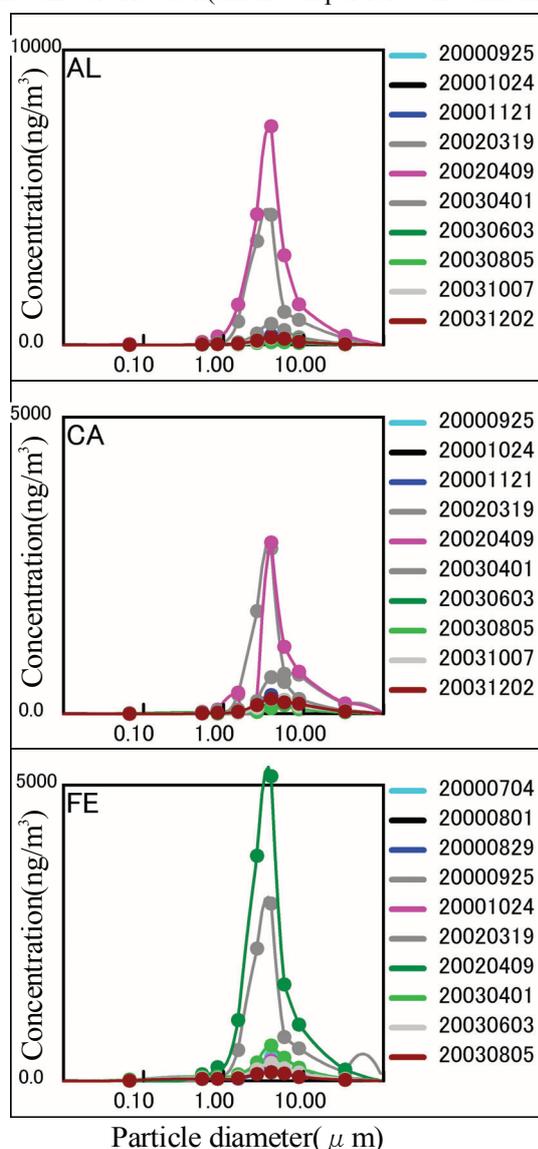

Fig.1 Size distribution of Al,Ca,Fe in the atmospheric aerosols observed at Sakai, 2000-2003.
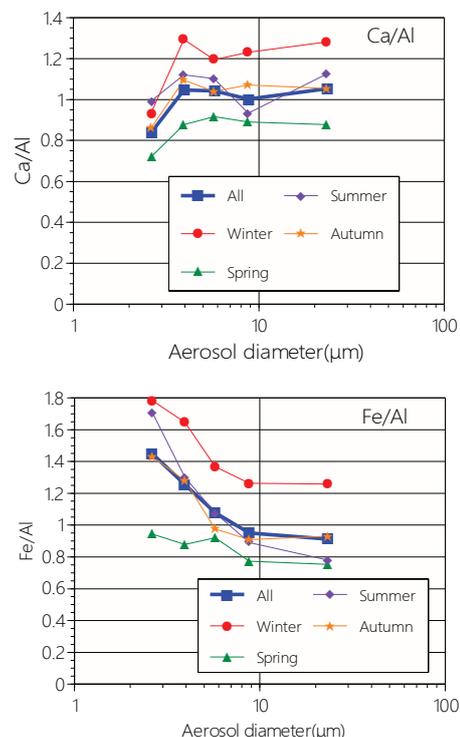

Fig.2 Change in ratio to Al of Ca and Fe by the particle size for all period and each seasons.

R2044

CO5-7 Mineral Luminescence and Application to Seismic Fault Geochronology

N. Hasebe, K. Miura[1], U. Uyangaa[1], Y. Igarashi[1], K. Oohashi[2], S.Akutsu[2], and Y. Iinuma[3]

Institute of Nature and Environmental Technology, Kanazawa University

[1] *Graduate School of Natural Science and Technology, Kanazawa University*

[2] *Graduate School of Science and Technology for Innovation, Yamaguchi University*

[3] *Institute for Integrated Radiation and Nuclear Science, Kyoto University*

INTRODUCTION: Luminescence dating observes the natural accumulated radiation damage caused by radioisotopes such as U and Th as the form of glow after stimulation by heating or lightening. Because of age range applicable, luminescence dating has been applied to Quaternary active fault (e.g., Ganzawa et al., 2013). However, little comprehensive studies on the effect of rock deformation or destruction through the faulting on luminescence signal have been reported so far. Oohashi et al. (2020) report the effect of faulting on the luminescence signal using quarts extracted from a granite sample. They gave a known radiation dose first, and artificially ground them to observe the behavior of luminescence sites during the faulting. They found frictional heating, that is controlled by the sample depth (normal stress), slip rate, and displacement length, is a major factor to reduce the luminescence intensity by the faulting. However, luminescence signal from the granitic quartz varies among quartz grains, causing a significant statistical uncertainty in the result. In this study, a sample with more stable luminescence signal was sought and an artificial grounding experiment was carried out to see the effect of starting material difference related to the difference in Geology.

EXPERIMENTS: Quartz were extracted from the sediment deposited on the beach, Kasado Island, Yamaguchi Prefecture. Conventional mineral separation processes were applied and luminescence characteristics were examined for quartz grains with the size of 150 -250 μm. Samples were wrapped with aluminum foil and irradiated at gamma-ray irradiation facility at KUR to give a known dose of 200 Gy. To check the initial status, some part of samples were brought to Kanazawa University and optically stimulated luminescence (OSL) was measured. Afterwards, samples were brought to Yamaguchi University and friction experiment to simulate fault activity was performed.

RESULTS: The quartz from Kasado inland mainly composed of fast and medium luminescence components (Fig. 1). Suitability of Kasado quarts in luminescence measurement was examined through preheat plateau test, dose recovery test and recycling ratio check (Fig. 2). When we estimated the amount of accumulated dose by luminescence measurement after the gamma irradiation, the accumulated dose was smaller than expected, and they are in the range of 0.4-17 Gy. This discrepancy may be caused by the different ionization efficiency between quartz and water, which is used to determine the dose distribution in the gamma irradiation facility. The frictional experiment resulted in the consistent behavior in luminescence signal decrease with the previous result (Oohashi et al., 2020), demonstrating that the luminescence signal decrease by faulting is a general phenomenon regardless of quartz source or luminescence component.
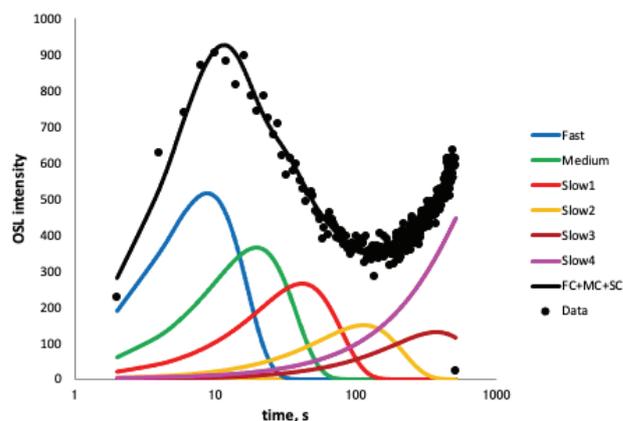

Fig. 1. Example of LM-OSL signal and the results of deconvolution.
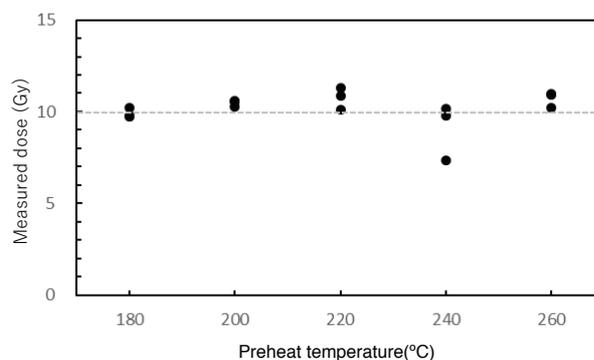

Fig. 2. Results of preheat plateau test

REFERENCES:

[1] Y. Ganzawa *et al.*, Jour. Geol. Soc. Japan, **119** (2013 714-726.

[2] K. Oohashi et al., JGR Solid Earth (2020) https://doi.org/10.1029/2020JB019900

R2049

CO5-8   Absorption of alkali metal ions by white radish sprouts (II)

M. Yanaga, S. Konagai[1], M. Hasegawa[1], H. Yoshinaga[2], R. Okumura[2] and Y. Iinuma[2]

Center for Radioscience Education and Research, Faculty of Science, Shizuoka University
[1]*Department of Chemistry, Faculty of Science, Shizuoka University*
[2]*Institute for Integrated Radiation and Nuclear Science, Kyoto University*

INTRODUCTION: According to a rumor damage survey on agriculture, forestry and fishery products in the disaster area conducted by the Consumer Affairs Agency in January 2021, 8.1% people still answered that they "hesitate" to purchase food from Fukushima Prefecture even though it has been about 10 years since the Fukushima Daiichi Power Plant accident occurred[1]. It seems that the damage caused by rumors will not disappear as long as radioactive substances remain in the field soil. Radioactive cesium is especially a problem because of its long half-life. However, simply removing the contaminated soil will result in a large amount of radioactive waste. Therefore, separating radioactive cesium from the soil is necessary to prevent damage by rumors and to minimize the quantity of radioactive waste.

Our previous reports have shown that the absorption of radioactive cesium from artificially contaminated soil into rice plants increased by adding a stable isotope to irrigation water and that the possibility that the cesium atoms added were replaced with radioactive cesium atoms in soil [2, 3]. However, addition of excess amount of stable cesium caused an obstacle to growth of rice plant [4]. Therefore, we recently conduct hydroponic culture of white radish sprouts and analyze trace elements contained in leaves and stems to investigate the behavior of cesium added to the culture solution and the competitive relationship between alkali metals.

EXPERIMENTS: *Materials and Method* Cultivation of white radish sprouts was carried out by adding alkali metal ions, such as potassium ions, rubidium ions and/or cesium ions, to a diluted solution of a commercially obtained culture solution, HYPONeX® (HYPONeX JAPAN CORP.,LTD.).

Seeds of white radish sprouts were soaked in ultrapure water and germinated in a dark place (1st day). The germinated white radish sprouts were transferred to a bright place, and 20 mL of culture solution diluted to 1/2000 concentration was added on 4th day. On 8th day, (Exp. 1) 20 mL of CsCl or RbCl aqueous solution ($1.0 - 30.0 \times 10^{-6}$ mol/L) or 20 mL of ultrapure water, or (Exp. 2) 20 mL of CsCl (20.0×10^{-6} mol/L), and 20 mL of KCl aqueous solution ($1.0 - 30.0 \times 10^{-6}$ mol/L) or 20 mL of ultrapure water, was added. Then, they were harvested on the 12th day.

INAA The samples in polyethylene capsules were irradiated in Pn-3 for 90 seconds and in Pn-2 for 4 hours, for short and long irradiation, respectively. As comparative standards, the certified NIST Standard Reference Mate-rial 1577b Bovine Liver as well as elemental standard for Cs was used. The γ-ray spectroscopic measurements with an HPGe detector were performed repeatedly for the short-irradiated samples: the first measurements for 120 – 900 seconds after decay time of 5 - 15 minutes and the second one for 250 - 1200 seconds after 60 - 150 minutes. The long-irradiated samples were measured for 1 - 24 hours after an adequate cooling time (15 - 60 days).

RESULTS: Previously, we reported that increasing the concentration of cesium ions in the culture medium caused leaf discoloration and growth disorders[5]. No such disorder was observed in the range of cesium ion concentration in Exp.1 of the present work. However, average manganese concentration in the leaves and stems of white radish sprouts grown with the addition of cesium ions was 19.1 ± 0.9 μg/g, whereas that with the addition of rubidium ions was 22.3 ± 0.5 μg/g. This suggests that the decrease in manganese concentration due to the addition of cesium ions may cause plant growth troubles.

Increasing the concentration of cesium or rubidium ions in culture medium increased the cesium or rubidium concentration in the leaves and stems. On the other hand, when the cesium ion concentration in the culture solution was kept constant and the potassium ion concentration was increased, the cesium ion concentration in the leaves and stems decreased (Exp. 2). This means that potassium ions suppress the absorption of cesium ions, or that potassium ions are more easily absorbed. However, no correlation was found between those effects and potassium ion concentration, and it depended only on the presence of potassium ions. In order to realize phytoremediation by adding stable isotope cesium, it is necessary to investigate furthermore the behavior of various essential elements such as potassium and manganese necessary for plant growth.

REFERENCES:
[1] Consumer Affairs Agency, Survey of consumer awareness regarding reputational damage (14th), https://www.caa.go.jp/notice/entry/023300/ [in Japanese].
[2] M. Yanaga *et al.*, NMCC ANNUAL REPORT, 22 (2015)185-190.
[3] M. Yanaga *et al.*, NMCC ANNUAL REPORT, 23 (2016)172-179.
[4] M. Yanaga *et al.*, KURNS Progress Report 2018 (2019)CO5-10.
[5] M. Yanaga et al., KURNS Progress Report 2019 (2020)CO5-9.

R2054

CO5-9 Study on the variation of the concentration of elements diffusing in the atmosphere by INAA

N. Hagura[1, 2], H. Matsuura[1, 2], T. Uchiyama[2], Y. Okada[2]

[1] *Nuclear Safety Engineering, Tokyo City University*
[2] *Atomic Energy Research Laboratory, Tokyo City University*

INTRODUCTION: Since 2002, sampling of airborne particulate matter have been performed on our facility, the Atomic Energy Research Laboratory of Tokyo City University (TCU-AERL). Even before that, studies on the measurement of radioactivity in the environment has been conducted, and the concentration distribution of Be-7 and Pb-210 and chemical forms in deposition have been analyzed [1]. These studies mainly focused on the biological characteristics of yellow sand that came to the Japanese archipelago. Samples are collected approximately every week. As partial example, Figure 1 shows the annual variation of atmospheric particulate matter (APM) concentration between 2011 and 2014 at TCU-AERL.

After the accident in Fukushima in March 2011, studies on the dynamics of radioactive cesium have been conducted [2, 3]. And we are also working on "Modeling of time series data of radioactive cesium concentration in lake water of Lake Onuma on Mt. Akagi [4]" and "Development of mathematical model for long-term prediction of radioactive cesium concentration in airborne particulate matter [5]" as a joint research program with Tsukuba University. These research themes have in common the elucidation of the dynamic behavior of cesium at low concentrations, and the neutron activation analysis method, which is a trace element analysis method, can serve as an important tool.

The sampled filters have been accumulated in the laboratory and are ready to be analyzed again. In this year we aimed to detect the trace elements by neutron activation analysis, targeting the samples from 2012 to 2014.

In the future, we plan to proceed with the analysis of a large number of samples in combination with the PIXE analysis method using the tandem accelerator at our facility (TCU-Tandem) [6], because it is impractical to analyze all samples by the Instrumental Neutron Activation Analysis (INAA) method.
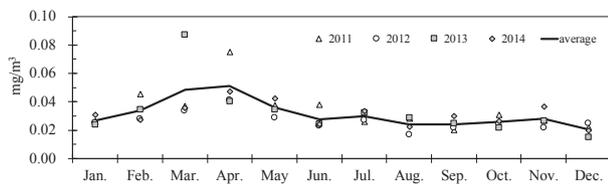

Fig. 1. Annual variation of APM concentration between 2011 and 2014 at TCU-AERL

EXPERIMENTS: We use a high volume air sampler (Shibata Scientific Technology LTD., HV-1000F, filter: ADVANTEC, QR-100 (collection efficiency: 99.99% for 0.3 μm particles)) with an inhalation flow rate of 700 L min^{-1}. The radioactivity of the filter that has collected dust is measured by a high-purity germanium semiconductor detector, and a part of the filter was stored for neutron activation analysis.

Irradiation was performed at the research reactor KUR at the Institute for Integrated Radiation and Nuclear Science, Kyoto University, between the November and December with four machine times in FY2020. The irradiation conditions are shown in Table 1. The measurement of radioactivity of short half-life nuclides was carried out using the HP-Ge semiconductor detector of the hot laboratory of KUR. And long and medium-lived nuclides, after cooling for one or two weeks, transported to the TCU-AERL, and was measured by a HP-Ge semiconductor detector. JLk-1 was used as a comparative standard substance.

Table 1. Irradiation conditions

Irradiation			Operating power	Thermal neutron flux
date	time	position		
2020/11/17	30 sec	Pn-3		4.7×10^{12} n/cm^2/sec
2020/12/1	60 min	Pn-2	1 MW	5.5×10^{12} n/cm^2/sec
2020/12/8	30 sec	Pn-3		4.7×10^{12} n/cm^2/sec
2020/12/15	60 min	Pn-2		5.5×10^{12} n/cm^2/sec

RESULTS: Focusing on the gamma-ray energy of 604 keV from Cs-134, the yearly cesium concentrations are discussed in Fig. 2. In this figure, the values for 2013 and 2014 are shown with respect to 2012. The error bars are the standard deviation of the variability of the seven samples for each year. This result shows that there is no significant difference in the amount of stable cesium sampled from year to year. We will continue to compare the trace elements contained in the filters.
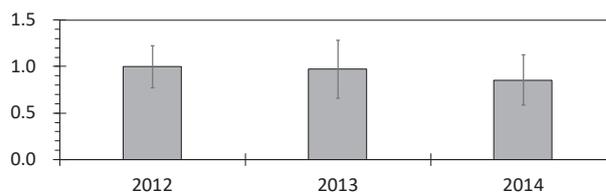
Fig. 2. Comparison of cesium concentration in 2013 and 2014 with respect to 2012.

REFERENCES:
[1] K. Hirose, et al., Atmospheric Environment, 38 (38), pp. 6601-6608 (2004).
[2] K. Nakamachi, et al., Bunseki Kagaku, 64 (8) pp. 589-594 (2015).
[3] N. Hagura, et al., Bunseki Kagaku, 66 (3), pp. 201-204 (2017).
[4] Y. Okada, et al., 6th Fukushima University IER Annual Symposium, P-129 (2020).
[5] E. Suetomi, et al., 6th Fukushima University IER Annual Symposium, P-130 (2020).
[6] N. Hagura, et al., Transactions of the Atomic Energy Society of Japan, 17 (3-4), pp. 111-117 (2018).

R2061

CO5-10 Neutron activation analysis of carbonate reference materials: coral (JCp-1) and giant clam (JCt-1)

S. Sekimoto, Y. Homura[a], V.D. Ho[1], M. Inagaki, N. Shirai[2], T. Ohtsuki

Institute for Integrated Radiation and Nuclear Science, Kyoto University
[1]Nuclear Research Institute, Vietnam Atomic Energy Institute
*[2]Department of Chemistry, Tokyo Metropolitan University*
[a]Present address: Novaltis Farma

INTRODUCTION: Geochemists are often interested in the abundance of halogen elements in geochemical materials such as crustal rocks, mantle materials, and meteorite samples, because halogens play an important role in investigating the petrogenesis of such materials and assist in tracing their origins and/or precursor materials [1-3]. In our previous work, radiochemical neutron activation analysis (RNAA) was refined to accurately determine even trace amounts of halogens (chlorine, bromine, and iodine) in sedimentary rock reference samples [4]. Subsequently, U.S. Geological Survey (USGS) geochemical reference materials were subjected to RNAA, and the data obtained were compared with literature data [5]. The two kinds of carbonate reference materials investigated here, JCp-1 (Coral) and JCt-1(Giant Clam), are prepared by the Geological Survey of Japan/National Institute of Advanced Industrial Science and Technology (GSJ/AIST), and the concentrations of many major and a few trace elements in these materials have been determined [6-8]. Data about the halogen contents in these materials is expected to significantly contribute to a better understanding of the chemistry of seawater and the marine environment, since halogens (especially iodine) are known to be extremely useful in investigating the geochemical circulation of terrestrial materials [9]. However, to our knowledge, there is not much data on the halogen contents of these carbonate materials.

The present study aims to use RNAA and instrumental NAA (INAA) to determine trace amounts of three halogens in JCp-1 and JCt-1, together with other elements. Based on the halogen data, the differences between the two carbonate reference materials is investigated. The INAA values obtained in the present study are compared with literature values, and the consistency between our data and the data from known literature is evaluated.

RESULTS: To probe the utility of the halogen data in interpreting geochemical formations, we have compared the halogen contents in these two carbonate materials with those in nine sedimentary rock materials (RNAA was used to determine the halogen content in all cases [4]). Since the carbonate materials contain CaO as the major component, the I/CaO and Br/CaO ratios in the two carbonates, as well as in the nine sedimentary rocks were determined and are shown in Fig 1. In spite of the fact that the CaO contents in the sedimentary rocks vary over a wide range (0.56% for JSd-3 (stream sediment) to 55.1% for JLs-1 (limestone)), the sedimentary rocks seem to exhibit a good correlation between these two ratios, except for JCh-1 (chert). As for the two carbonate reference materials, JCp-1 (Coral) also shows a reasonable correlation between the two ratios, implying that fractionation between Br and I may not have occurred in the formation of a coral like JCp-1 and the sedimentary rocks, except for JCh-1. On the other hand, JCt-1 (Giant Clam) clearly does not exhibit such a correlation, suggesting the possibility of fractionation of I from Br during its formation.
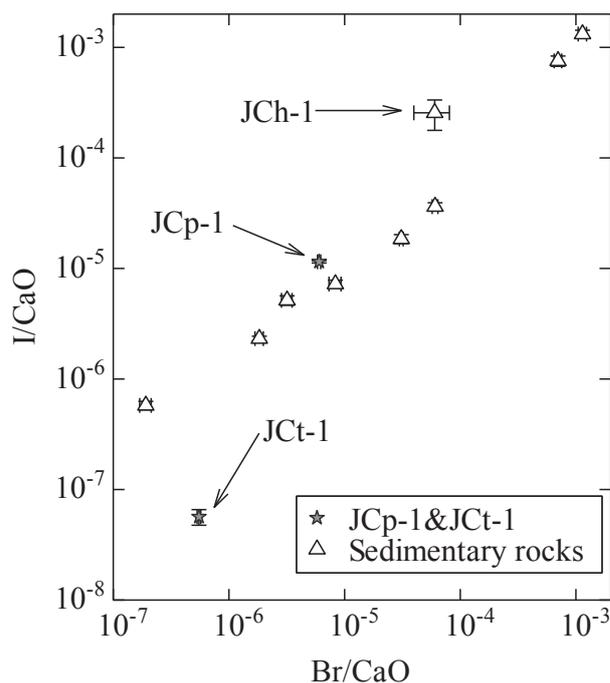
Fig. 1 I/CaO vs. Br/CaO ratios for JCp-1, JCt-1 and sedimentary rocks.

REFERENCES:
[1] MA Kndrick *et al.*, Geochim. Cosmochim. Acta **235** (2018) 285-304.
[2] L. Hughes *et al.*, Geochim. Cosmochim. Acta **243** (2018) 1-23.
[3] DE Harlov *et al.*, The Role of Halogens in Terrestrial and Extraterrestrial Geochemical Processes Springer Geochemistry, Gewerbestrasse, Switzerland (2018)
[4] S. Sekimoto *et al.*, Anal. Chem. **85** (2013) 6336-6341.
[5] S. Sekimoto *et al.*, Geostand. Geoanal. Res. **41** (2017) 213-219.
[6] S. Aizawa, J. Radioanal. Nucl. Chem. **278** (2008) 349-352.
[7] M. Inoue *et al.*, Geostand. Geoanal. Res. **28** (2004) 411-416.
[8] T. Okai *et al.*, Chikyuukagaku **38** (2004) 281-286.
[9] B. Deruelle et al., Earth Planet. Sci. Lett. **108** (1992) 217−227.

R2077

CO5-11　　　　　　　**^{40}Ar-^{39}Ar Dating of Extraterrestrial Materials in KURNS**

N. Iwata, S. Sekimoto[1], R. Okazaki[2] and Y. N. Miura[3]

Faculty of Science, Yamagata University
[1]Institute for Integrated Radiation and Nuclear Science, Kyoto University
[2]Department of Earth and Planetary Sciences, Kyushu University
[3]Earthquake Research Institute, University of Tokyo

INTRODUCTION: Radiometric dating is useful tool for unveiling formation and evolution process of planetary material. ^{40}Ar-^{39}Ar method is invaluable to date the timing of heating events on planetesimal and asteroid (e.g. Swindle et al. (2014) [1]). Especially, ^{40}Ar-^{39}Ar dating method with laser heating technique is suitable for small amount sample (e.g. Kelley, 1995 [2] and Hyodo, 2008 [3]).

For example, tiny material returned from asteroid 25143 Itokawa is dated using laser heating ^{40}Ar-^{39}Ar dating method by Park et al. (2015) [4] and Jourdan et al. (2017) [5]. Park et al. (2015) reported an age of 1.3 ± 0.3 Ga. Jourdan et al. (2017) reported an age of 2.3 ± 0.1 Ga. These ages indicate the timing of catastrophic events which were occurred on Itokawa's precursor body. Combining the ^{40}Ar-^{39}Ar ages and other chronological data, Terada et al. (2018) [6] overviewed the time evolution of the Itokawa asteroid. Similar investigation, the integration of multichronological data is proposed to the material that recovered from asteroid 162173 Ryugu and other extraterrestrial materials. ^{40}Ar-^{39}Ar dating will play an important role within the investigations.

To implement of dating of extraterrestrial material by ^{40}Ar-^{39}Ar method, we will develop a system which includes gas extraction and gas purification line in KURNS (Fig. 1).

EXPERIMENTS: Dr. R. Okazaki of Kyushu University designed the system. Fig.1 shows schematic diagram of the system. A continuous Nd-YAG laser (~60 W) extract gas from neutron irradiated sample. The extracted gas is purified using a Sorb-AC getter pump in purification part. Gas trap tree consists of several metal gas traps. The purified gas is encapsulated into metal gas trap (CH) in gas trap tree part. The purified gas in the metal gas trap is transported to laboratories of noble gas analysis (e.g. Kyushu University), and then, argon isotope of the gas is analyzed using noble gas mass spectrometer. Whole of the extraction and purification parts are evacuated by two oil rotary pumps, two turbo molecular pumps and an ion pump to ultra-high vacuum condition.

We have a plan to connect a quadrupole mass spectrometer (QMS) to this system, to perform on-lined laser heating ^{40}Ar-^{39}Ar dating in future.

RESULTS: We started assembling of the laser-heating gas extraction and purification system in KURNS in 2019. The design work and configuration of the system is almost completed in 2020. We are going to continue setting the system up during 2021.

REFERENCES:
[1] T. D. Swindle *et al.*, in *Advances in ^{40}Ar/^{39}Ar Dating: from Archaeology to Planetary Sciences*, edited by Jourdan, Mark, Verati (Geol. Soc., London, Spec. Pub. **378**, 2014) 333-347.
[2] S. P. Kelley, in *Microprobe techniques in the earth sciences*, edited by Potts, Bowles, Reed, Cave (Chapman & Hall, London, 1995) 327-358.
[3] H. Hyodo., Gondwana Res. **14** (2008) 609-616.
[4] J. Park *et al.*, Meteorit. and Planet. Sci., **50** (2015) 2087-2098.
[5] F. Jourdan *et al.*, Geology, **45** (2017) 819-822.
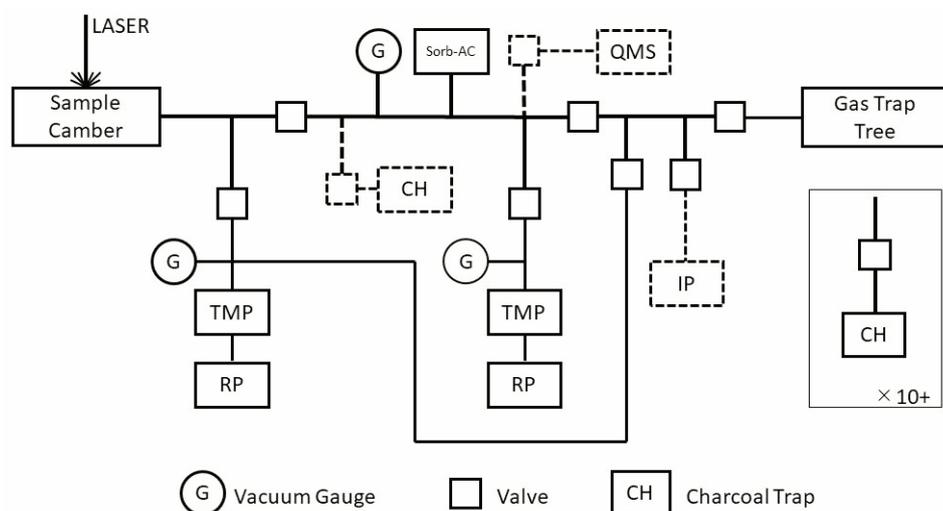[6] K. Terada *et al.*, Sci. Rep., **8** (2018) #11806.

Fig. 1. Schematic diagram of gas extraction and purification line in KURNS. RP, TMP, IP and QMS respectively denotes rotary pump, turbo molecular pump, ion pump and quadrupole mass spectrometer. Components with dashed line are connected during 2021.

Neutron Activation Analysis of Iron Meteorites

N. Shirai[1], S. Sekimoto[2]

[1]*Department of Chemistry, Tokyo Metropolitan University*
[2] **Institute for Integrated Radiation and Nuclear Science, Kyoto University**

INTRODUCTION: Iron meteorites are made of FeNi metal phases with such minor minerals as schreibersite, troilite, and cohenite. Most iron meteorites are considered to be samples of metallic cores and pools that formed in small planetary bodies, petrological, mineralogical and chemical studies of iron meteorites are fundamental for unraveling the processes of planetary differentiation. Iron meteorites are classified into 13 groups based on their structure and chemical compositions [1]. Iron meteorites which do not fit into an established group are described as ungrouped. The structural classification is based on the presence or absence of the Widmanstätten pattern, which develops as a two-phase intergrowth of kamacite and taenite. Chemical classification is based on the abundances of trace elements (Ga, Ge and Ir). Traditionally, Ni was used as the independent variable in classifying iron meteorites. Recently, Au has been used due to a much better estimate of a meteorite's position within the fractional crystallization [2]. In this study, our analytical procedure of INAA for iron meteorites [3] was modified so that it can be applied to the new chemical classification. Based on the analytical results, accuracy of our data obtained by using the modified procedure and how promisingly our analytical method can be applied to classification of iron meteorites.

EXPERIMENTS: Odessa (IAB-MG), Canyon Diablo (IAB-MG), Cape York (IIIAB), Muonionalusta (IVA) and Dronino (ungrouped) iron meteorites were analyzed in this study. These iron meteorites were sawn into plate roughly 1 x 4 x 4 mm in size by using a ISOMET low speed saw. After cutting, each iron meteorite was cleaned by sandpaper. Then, iron meteorites were washed in ultrasonic bath by using acetone. The analytical procedure used in this study is basically similar to that described by Shirai et al. [3]. Sample was irradiated for 10 sec. at the pn-3 of Institute for Integrated Radiation and Nuclear Science, Kyoto University, Kyoto with thermal and fast neutron fluxes of 4.6 x 10^{12} and 9.6 x 10^{11} cm^{-2}s^{-1}, respectively. After irradiation, sample was immediately measured for gamma-ray emissions for the determination of Co, Ni, Cu, Ge and Rh. After one day cooling, sample was measured for gamma-ray emissions for the determination of Fe, Co, Ni, Ga, As, W, Ir and Au. Chemical standards were prepared from high-purity chemical reagents for the elements of interest. For Fe, Co and Ni, metal was used. For the other elements, single-element standard solution for atomic absorption analysis was used. These single-element standard solutions were separately prepared by dropping known concentration of these ele-ments on the filter papers.

RESULTS: For all iron meteorites analyzed in this study, five elements (Fe, Co, Ni, Cu, Rh and Au) could be detected. Our values for these elements are in good agreement with the corresponding literature values [4-6]. In contrast, Ge and Ge in Muonionalsuta and Dronino, As in Dronino, W in Cape York, Muonionalusta and Dronino and Ir in Muonionalusta could not be detected due to their low concentrations.

Gallium abundances for iron meteorites are plotted against Au abundance in Fig. 1. Our data for Odessa and Canyon Diablo, and Cape York are plotted in the field of IAB and IIIAB, respectively, indicating that these iron meteorites are classified into IAB and IIIAB. Our observations are consistent with the previous studies [4-6]. The detection limit of the modified analytical procedure is about 10 ppm of Ga. Except for some IAB, IIF, IIIF, IVA and IVB, Ga abundances for the most iron meteorites can be determined by using the modified analytical procedure. The detection limit obtained in this study is 17 times higher than those in the previous study [3]. In the analysis of iron meteorites with having less than 10 ppm of Ga, iron meteorite is reirradiated for 4 hrs at the pn-2 [3] or other elements such as Ir can be used for the classification of iron meteorites. It is concluded that our modified analytical procedure of INAA is more simple than the previous procedure [3].
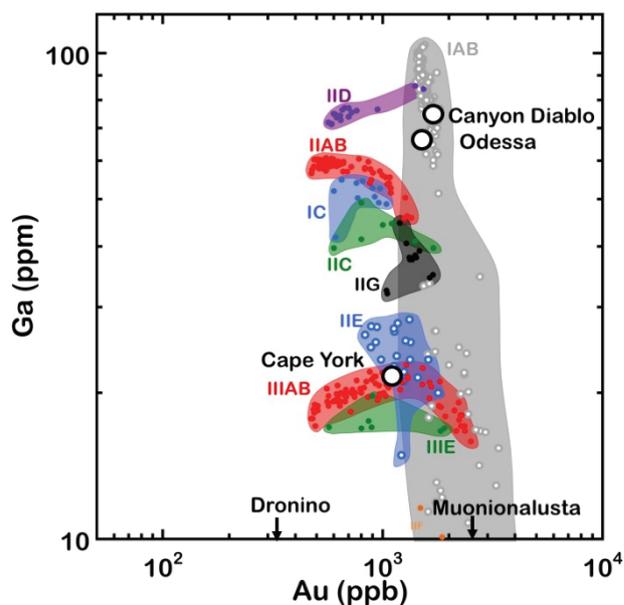
Fig. 1. Au abundances versus Ga abundances for iron meteorites.

REFERENCES:
[1] J. I. Goldstein *et al.*, Chem. Erde., **69** (2009) 293-325.
[2] J. T. Wasson *et al.*, Geochim. Cosmochim. Acta **62** (1998) 715-724.
[3] N. Shirai *et al.*, J. Radioanal. Nucl. Chem., **303** (2015) 1375-1380.
[4] J. T. Wasson, Geochim. Cosmochim. Acta **63** (1999) 2875-2889.
[5] J. T. Wasson and J. W. Richardson, Geochim. Cosmochim. Acta **65** (2001) 951-970.
[6] J. T. Wasson and G. W. Kallemeyn, Geochim. Cosmochim. Acta **66** (2002) 2445-2473.

R2083

CO5-13   Neutron activation analysis of stable cesium and trace elements in the lake water of Lake Onuma on Mt. Akagi

Y. Okada [1], N. Kumagai [2], T. Uchiyama [1], N. Hagura [3], H. Matsuura [3] and Y Iinuma [4]

[1]*Atomic Energy Research Laboratory, Tokyo City University*
[2]*Cooperative major in Nuclear Energy, Tokyo City University*
[3]*Department of Nuclear Safety Engineering, Tokyo City University*
[4] *Institute for Integrated Radiation and Nuclear Science, Kyoto University*

INTRODUCTION: Lake Onuma on Mt. Akagi in Gunma Prefecture has been confirmed to be contaminated by radioactive Cs due to the accident at the Fukushima Daiichi Nuclear Power Plant in 2011. We have been investigating the lake for the past eight years, but the decrease in the concentration of radioactive Cs in the lake water and in the inhabiting pond smelt has been very slow[1,2] . In order to investigate the cause of this, we analyzed trace elements in sediments and phytoplankton last year. In this study, trace elements in the lake water were analyzed by neutron activation analysis. From these results, we aim to derive the relationship between trace elements and the movement of radioactive Cs in Lake Onuma.

EXPERIMENTS: Samples were collected at depths of 0 m, 8 m and 15 m in 2018 and 2019. Two types of lake water samples were collected untreated samples (bulk samples) and filtered through a 0.45 µm filter (soluble form). Approximately 500 mL of each sample was freeze-dried. 27 samples (approximately 1 mg to 2mg of drying weights) and reference standard materials (JLk1,NIES8) were irradiated with KUR Pn3 (thermal neutron flux: 4.68×10^{12} /ncm^{-2}/ s^{-1}) for 30s, followed by cooling for 3 to 5 min, and ɤ-ray measurements were performed. In addition, was irradiated with KUR Pn2 (thermal neutron flux: 5.5×10^{12}/ ncm^{-2} /s^{-1}) for 1 hour, followed by cooling for 7to 14 days, and ɤ-ray measurements were performed. The analysis was carried out using software (Gamma Studio : SEIKO EG &G Co.). The analytical values for the particle form were obtained by subtracting the value for the soluble form from the analytical value for the bulk sample.

RESULTS: Seventeen elements (Al, Mg, Mn, Na, Fe, V, Ca, K, Sc, Cr, Co, Zn, Rb, Sb, Cs, Ba and Ce) in the lake water were measured by neutron activation analysis. The results showed that Cs and Rb were detected in all samples. The elements detected in the bulk samples were Al, V, Mg, and Ca. In addition, Fe, Mn, and Cr were detected in bulk samples and soluble forms collected in August 2018.

Figure 1 shows the concentrations of stable Cs at 0, 8, and 15 m depth in the lake. The concentration of stable Cs in the bulk samples varied from 0.1 µg/L to 0.4 µg/L at water depths of 0, 8, and 15 m. It was found that the surface layer at 0 m contained more cesium in the particle form than in the soluble form, regardless of the season.

Research on radioactive cesium in lake water has been conducted since 2012. As a result, we found that the concentration of soluble forms radioactive cesium increases in summer in the deep layer of 15m depth. This time, the same result was obtained for stable cesium in the lake water.

In Lake Onuma, a water temperature dynamic layer is formed within the lake bottom during the summer, which is divided into a surface layer and a deep layer. In the
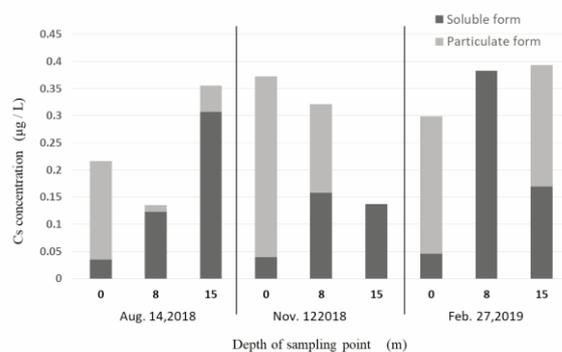

Fig. 1 Stable cesium concentration of lake water in Lake Onuma

deep layer, oxygen depletion phenomenon occurs. In this study, 1.2 mg/L of Fe and 0.77 mg/L of soluble forms Fe were detected in the 15 m bulk in Aug. 2018. These results suggest that the deep water is in a reducing state during the summer. It was suggested that the reducing state was related to the increase in soluble forms Cs. The concentration of Rb, the same alkali metal, varied in the range of 0.7 µg/L to 2.5 µg/L. Similar to Cs, Rb was found to be more abundant in soluble form in August. Looking at the concentration of K, the same alkali metal, 0.04 µg/L to 0.06 µg/L was contained in the soluble form, and no seasonal variation was observed.

In the future, it will be necessary to consider the material balance.

REFERENCES:
1)   M.Mori,K.Tsunoda, *et al*., Sci. Total Envron., **575**,1247-1254 (2017).
2)   K.Suzuki, S.Watanabe*et, al.*, Sci. Total Envron., **622**,1153-1164 (2018).

R2092

CO5-14   **Transfer of silver, cesium, and rubidium from nutrient solution to radish (*Raphanus sativus* var. sativus)**

T. Kubota, S. Fukutani, and Y. Shibahara

Institute for Integrated Radiation and Nuclear Science, Kyoto University

INTRODUCTION: Silver-110m is one of the radionuclides that is significantly detected in the environmental samples after the accident of the Fukushima Dai-ich nuclear power plants [1]. Its effect on internal exposure was insufficiently reported compared to other major radionuclides, such as cesium-137. Evaluations of internal exposure require various environmental parameters. Among them, the transfer behavior of radionuclides to and inside editable plants, radish (*Raphanus sativus* var. sativus), was investigated under hydroponic condition. Besides of radioactive silver and cesium, radioactive rubidium was added to compare their transfer behavior.

EXPERIMENTS: Silver-105, cesium-136, and rubisium-83 used as tracers were produced through photo nuclear reaction at KURNS-LINAC and purified by precipitation and ion chromatography [2]. Radish samples were cultivated from seed in non-radioactive nutrient solution [3] for four weeks and then were replaced to fresh nutrient solution containing above radionuclides followed by cultivation for one, three, and five days. After each cultivation time, the root was washed by reverse-osmosis water and the washing solution was returned to its original nutrient solution. The cultivated sample was divided into three parts, root, radish, and leaf to be dried at 75 ºC for more than 12 hours. The radioactivity of dried samples and nutrient solution was measured by γ-spectrometry to determine the transfer and distribution ratio of three elements.

RESULTS: The transfer ratio of silver from nutrient to plant saturated at only one day, which was different from cesium and rubidium in Table 1. However, the ratio reached at most 60%. The transfer tendency of cesium was similar to rubidium while the ratio was smaller than rubidium. The distribution ratio of radionuclides between root and whole plant body was constant over cultivation time in Table 2. Silver almost completely remained in root and hardly moved to other parts. Even though the total amount of cesium and rubidium in the whole plant body increased as seen in Table 1, it is interesting that the distribution ration of those was constant. The distribution ratio of cesium and rubidium between radish and whole plant body decreased with cultivation time in Table 3. On the contrary, the distribution ratio of those between leaf and whole plant body increased in Table 4. This opposite tendency would be ascribed to the difference of the translocation rate of root to radish and radish to leaf. The same transfer tendency of silver between radish and lettuce (*Lacutuca sativa* var. crispa) [4] suggests that silver uptaken through root surface is one of elements that are

unlike to translocate from root to other plant parts.

Table 1 Transfer ratio of radionuclides from initial nutrient solution to plant

Day	^{105}Ag	^{136}Cs	^{83}Rb
1	0.56	0.05	0.11
3	0.62	0.15	0.32
5	0.56	0.33	0.61

Table 2 Distribution ratio of radionuclides between root and whole plant body

Day	^{105}Ag	^{136}Cs	^{83}Rb
1	0.96	0.24	0.15
3	0.96	0.24	0.15
5	0.95	0.26	0.15

Table 3 Distribution ratio of radionuclides between radish and whole plant body

Day	^{105}Ag	^{136}Cs	^{83}Rb
1	0.01	0.22	0.31
3	0.01	0.19	0.24
5	0.02	0.10	0.16

Table 4 Distribution ratio of radionuclides between leaf and whole plant body

Day	^{105}Ag	^{136}Cs	^{83}Rb
1	0.01	0.47	0.49
3	0.03	0.58	0.61
5	0.03	0.64	0.70

REFERENCES:
[1] K. Saito *et al.*, J. Env. Rad., **139** (2015) 308 - 309.
[2] T. Kubota *et al*., KURNS Progress Report (2018) 209.
[3] K. Fujiwara *et al*., Jpn. J. Health Phys., **50** (2015) 189 - 193.
[4] K. Iwata *et al*., Proc. 18th Workshop on Environmen-tal Radioactivity, (2017) 163-166.

R2098

Neutron Activation Analysis of Environmental Samples

Y. Oura and Md. S. Reza

Graduate School of Science, Tokyo Metropolitan University

INTRODUCTION: Environmental pollution is an important issue for our healthy life. Determination of elemental composition is one of the ways for an environmental examination. For example, shellfish are commonly used for an assessment of ocean environment. In this case soft tissues in shellfish (e.g., mussels) are mainly analyzed for elemental concentration, whereas shells seem not to be analyzed. Thus, we tried to determine elemental concentrations in shell if they are effective in assessing the coastal/lake environment. In this work, Japanese basket clam (scientific name: corbicula japonica) living in brackish-water lake was selected because it is easily available, and it has an easily handled size. For atmospheric environment, attention has been focused on the effects of very small particles called PM2.5 on human health in recent year. Elemental composition of particulates plays an important role for estimation of their origins. We have collected PM2.5 particulates at Hachioji, Tokyo and determination of elemental concentration in PM2.5 particulate has been continued since 2018.

EXPERIMENTS:
Shells
Japanese basket clam (Yamato Shijimi) yielded at different four lakes were got from a supermarket. After discarding soft tissues, clamshells were cleaned properly by ultrapure water using an ultrasonic water bath. Then they were made powder after drying. Shells of two individuals were made powder together to prepare a sample. Five samples (total 10 individuals) were subjected to analysis for each lake. About 180 mg of each sample was irradiated together with reference materials (GSJ JCp-1, JCt-1, and JB-1a) for 30 seconds and 4 hours at KUR (1 MW operation). After irradiation gamma-rays were measured by HPGe detector.

PM2.5
PM2.5 particulates have been collected on a Nucleopore polycarbonate filter with 0.2 µm of pore size for three weekdays every week at a rooftop of a building in Minami-Osawa campus of Tokyo Metropolitan University. Polycarbonate filters on which PM2.5 was collected were cut in half, then one half was subjected to analysis. Filter sample in clean polyethylene bag was irradiated together with reference materials (NIST 1648, NIST 1632c, NIES No.8, and GSJ JB-1a) for 5 minutes at KUR (1 MW operation) and 1 hour at KUR (5 MW operation). After irradiation, gamma-rays were measured by Ge detector.

RESULTS:

Shells

Shijimi shells in four different lakes (in Hokkaido, Aomori, Ibaraki, and Shimane) were analyzed and eight elements (Na, Ca, Mn, Fe, Zn, Br, Sr, and Ba) were determined. Mean elemental concentrations of 5 determination values for each location (H, A, I, and S) are shown in Fig.1 together with standard deviations expressed by error bars. Calcium is the most abundant element among determined elements because shell is calcium carbonate, thus no deviations of concentrations are observed in 20 samples. And Na, Zn, and Sr concentrations are also less deviation. For Fe, large deviation was observed in 5 samples of each 4 location, but the average values are almost consistent. On the other hand, the mean values of Mn and Ba for 4 locations are varied. Although Ba is a homologous element of Ca and Sr, a behavior of Ba is possibly different from that of Ca when shell production. And it is interesting to see if Mn is a kind of environmental indicator.
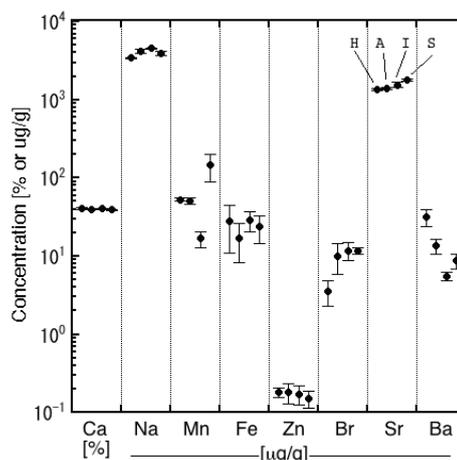

Fig. 1. Means of elemental concentrations in shells yielded in different lakes. Error bars express standard deviations of 5 samples for each lake.

PM2.5
Mass concentrations of PM2.5 particulates collected in FY2020 (Jan. to Sep.) ranged from 3 to 22 µg m^{-3}, and their median of 12 µg m^{-3} was almost same as the median in 2018 and 2019. Determined elemental concentrations in PM2.5 particulates collected in 2020 are compared to those in 2018 and 2019. The median values of elemental concentrations in 2018 and 2019 are similar in general like the mass concentrations. Atmospheric environment around our university seems not to be different yearly among in 2018, 2019, and 2020 on the average.

R2103

I-Xe ages of solar noble gas-rich meteorites

H. Sumino, K. Arai[1], S. Tachibana[1], J. Ren,
A. Takenouchi[2], M. Koike[3], R. Okumura[4], Y. IInuma[4],
H. Yoshinaga[4] and S. Sekimoto[4]

Graduate School of Arts and Sciences, University of To-kyo
[1]*Graduate School of Science, University of Tokyo*
[2]*National Institute of Polar Research*
[3]*Graduate School of Advanced Science and Engineering, Hiroshima University*
[4]*Institute for Integrated Radiation and Nuclear Science, Kyoto University*

INTRODUCTION: During the formation of planets from nebula gas and dust composing protoplanetary disk in the early solar system, the activity of the primordial sun increased at a certain period, and a large amount of nebula gas was blown away from the planet formation region by the strong solar wind. The lifetime of protoplanetary disk gas ranges 1-10 million years, which depends on viscous dissipation and photo-evaporation of the disk gas. It is not clear how long the Sun's protoplanetary disk held its gas component, during which gas giants formed. Ca-, Al-rich inclusions and chondrules are considered to have formed in the presence of disk gas, but the timing of clearing of disk gas has not yet been tightly constrained [1]. Bajo [2] found a correlation between Solar-wind derived noble gas concentrations and I-Xe ages of brecciated chondrites. Bajo [2] hypothesized that the I-Xe ages, which could represent impact ages [3], of solar-wind-rich meteorites indicated the timing of disk-gas clearing because the solar wind reaches to the surface of small bodies only after the complete dissipation of disk gas. In this study, to test this hypothesis, I-Xe ages and solar-wind noble gas concentrations of Zag (H36) and Northwest Africa 801 (CR2) (NWA 801) meteorites were determined.

EXPERIMENTS: About 30 mg fragments of these meteorites, irradiated with neutrons at the Kyoto University research reactor, were heated in vacuum stepwise in the temperatures range of 400-1800°C to extract xenon isotopes, including naturally-occurring radiogenic ^{129}Xe derived from ^{129}I and ^{128}Xe produced from ^{127}I by (n, β) reaction in the reactor. After purifying the noble gases extracted at each heating step, xenon isotope ratios were measured using a magnetic-sector-type mass spectrometer VG3600 [4]. The obtained ^{129}Xe/^{128}Xe ratios of the samples after corrections for low-temperature alteration and trapped component were converted to relative I-Xe ages by comparing with ^{129}Xe/^{128}Xe ratio of the Shallowater meteorite standard and was irradiated with neutrons together with the samples. About 5 mg fragments of the same meteorite specimen were heated in vacuum at 800 and 1700°C for naturally-occurring noble gas analysis to determine concentrations of solar-wind-derived noble gases.

RESULTS: The obtained ^{129}Xe/^{128}Xe ratios of the samples after corrections for low temperature alteration and trapped component were converted to relative I-Xe ages by comparing with ^{129}Xe/^{128}Xe ratio of the Shallowater meteorite with the absolute age of 4.5633±0.0004 billion years [5]. Although our new I-Xe ages are associated with relatively lager errors compared to those reported in [2] due to less neutron fluence to produce ^{128}Xe, two samples from the solar-wind-poor portion of Zag was systematically older (4.551 ± 0.008 and 4.558 ± 0.013 billion years) than those from the solar-wind-rich portion (4.554 ± 0.009 and 4.551 ± 0.006 billion years), which are consistent with the previous research [2]. The weighted mean of I-Xe ages of the solar-wind-poor and solar-wind-rich portions are 4.557 ± 0.004 and 4.550 ± 0.002 billion years (errors are 95% confidence levels), respectively, suggesting that solar nebular gas dissipation would have occurred between these ages. NWA 801, which is also a solar-wind-rich meteorite, yielded I-Xe age of 4.529 ± 0.016 billion years. The present dataset is broadly consistent with the hypothesis [2] and suggests that the timing of gas dispersal in the Sun's protoplanetary disk would be ~10 million years after the first solid formation (CAI condensation, 4.56730 ± 0.00016 billion years [6]), but further data with lesser analytical uncertainties is surely required.

REFERENCES:
[1] I. Pascucci and S. Tachibana, in *Protoplanetary Dust*, edited by D. Apai and D. S. Lauretta (Cambridge University Press, 2010).
[2] K. Bajo, Ph.D. Thesis, Univ. Tokyo (2010).
[3] J. D. Gilmour and M. J. Filtness, Nature Astronomy, **3** (2019), 326-331.
[4] Ebisawa *et al.*, J. Mass Spectrom. Soc. Jpn., **52** (2004) 219-229.
[5] J. D. Gilmour *et al.*, Meteorit. Planet. Sci., **41** (2006), 19-31.
[6] Connelly J.N. *et al.*, Science, **338** (2012) 651-655.

R2112

Bulk Chemical Compositions of two LL7 Chondrites

M. Ebihara, Y. Hidaka, J. Sakuma, A. Ueda, S., N. Shirai[1] and S. Sekimoto[2]

Department of Earth Science, Waseda University
[1]*Department of Chemistry, Tokyo Metropolitan Univ.*
[2]*KURNS*

INTRODUCTION: Chondrites are acknowledged to be the most primitive materials accessible to us for studying the early history of our solar system. Chondrites are grouped into three major chemical groups, carbonaceous, ordinary and enstatite chondrites, and into six petrological groups, types 1 to 6. Ordinary chondrites account for more than 80 % of meteorites. Most ordinary chondrites are petrographically classified into type 3 (more primitive and unequilibrated) to type 6 (differentiated and equilibrated). With further thermal alteration during the early differentiation process, chondrites were transformed to primitive achondrites with partly melting and, then, to achondrites, which had experienced melting and, eventually, lost the primitiveness. In this study, we studied chemical compositions of ordinary chondrite samples classified as LL7. Here, "LL" means that these samples contain low metals and low iron and "7" means that they were highly thermally altered but not totally melted. Type 7 chondrites were first proposed by Dodd et al. [1] for such meteorites which experienced higher degree of thermal alteration than that for type 6 (or less metamorphosed) chondrites. So far, 68 meteorites are classified into LL7 ordinary chondrites (Meteoritical Bulletin). Type 7 meteorites are believed to be "bridges" between chondrites and achondrites. In this study, two LL7 chondrites were analyzed for their elemental compositions by means of instrumental neutron activation analysis (INAA). Our goal is to understand the material differentiation process at the early solar system, especially a transient process from type 6 chondrites to primitive achondrite and further to achondrites.

EXPERIMENTS: Bulk chemical compositions of two LL7 chondrites (Y-790144 and Y-791067) have been determined by INAA. Several chips of each meteorite weighing 400-600 mg were powdered in a clean agate mortar. A portion (30-40 mg) of each powdered meteorite was used for INAA. Each meteorite sample doubly sealed in plastic bags was irradiated with neutron firstly for 10 s for determining elements using short-lived neutron-induced radionuclides. The same sample was irradiated secondly for 4 h for determining elements using long-lived nuclides. Quantification was done by comparison method using JB-1 (basaltic powder sample) and the Smithsonian Allende meteorite powder as reference samples. Gamma-ray spectrometry was done at KURNS for short-lived nuclides and Tokyo Metropolitan University for long-lived nuclides.

RESULTS: The INAA results are summarized in Table 1. Note that these data are preliminary at this stage. Numerical values of element contents were determined for 15 elements and upper limits were obtained for 12 elements. Compared with LL chondrite means, the two LL7 chondrites were depleted in Ca, Al and V. These elements were determined by using short-lived nuclides, which could be related to systematically low contents. Although our results are mostly consistent with literature values [2, 3], some inconsistency was observed. Besides INAA, ICP-MS was performed for rare earth elements. Based on INAA and ICP-MS data, cosmochemical discussion is to be held.

Table 1 Preliminary results obtained by INAA*

	. -790144	. -791067
Na(%)	0.686±0.016	0.639±0.017
Mg(%)	11.7±0.6	11.0±0.7
Al(%)	0.793±0.056	0.728±0.057
Ca(%)	0.565±0.222	0.906±0.252
S.(..)	7.84±0.8	8.15±0.08
V(..)	41.8±8.0	27.3±8.3
Cr(ppm)	3741±15	4006±16
Mn(%)	0.209±0.007	0.223±0.008
Fe(%)	20.6±0.1	19.5±0.1
Co(ppm)	501±3	302±2
Ni(%)	0.902±0.019	0.650±0.016
Zn(ppm)	<112	<111
Br(ppm)	<0.876	<0.866
Sb(ppb)	<231	<216
Ba(ppm)	<155	<147
La(ppb)	354±97	370±100
Sm(ppb)	259±25	208±25
Eu(ppb)	<264	<266
Gd(ppb)	<622	<598
Yb(ppb)	<500	<471
Lu(ppb)	<77.5	<73.3
Hf(ppb)	<978	<895
Ta(ppb)	<841	<722
Ir(ppb)	387±15	239±13
Au(ppb)	138±7	88.8±6.3
Th(ppb)	<886	<841
U(ppb)	<1679	<1501

*Uncertainties are due to counting statistics (1s). Upper limits are defined as 10s.

REFERENCES:
[1] R. T. Dodd et al. Geochim. Cosmochim. Acta **39** (1975) 1585-1594.
[2] J. M. Friedrich et al. Geochim. Cosmochim. Acta **139** (2014) 83-97.
[3] T. Yoshioka. 修士論文 (首都大学東京) (2016) .

R2113

CO5-18   Metamorphic age of Acasta gneiss and regional cooling history

H. Hyodo[1], K. Sato[1,2,3], H. Kumagai[3]and K. Takamiya[4]
[1] *Institute of Frontier Science and Technology,*
  Okayama University of Science
[2]*Department of Applied Chemistry and Biochemistry,*
  National Institute of Technology, Fukushima College
[3] *Submarine Resources Research Center Japan Agency*
for Marine-Earth Science and Technology
[4] *Institute for Integrated Radiation and Nuclear Science,*
Kyoto University

INTRODUCTION: Biotite age of Acasta gneiss is reported as 1.935 Ga [1], which gives large difference from U-Pb zircon SHRIMP age of 4.0 Ga [2]. The results from other samples suggest the biotite age is regional, and it seem to be consistent with U-Pb apatite age (1.9 Ga) [3].

Typical minerals in K-Ar system such as hornblende and biotite have its own diffusion characteristics which provide regional temperature at specific timing of cooling orogen.

EXPERIMENTS: Experimental procedure is the same as described as previous studies on single grain datings. Rock samples were crushed and sieved in #25-100 mesh. After ultrasonic cleaning in distilled water, single mineral grains were handpicked. The mineral grains were irradiated using the hydraulic facility of KUR for 47 hours at 1 MW, and subsequently 6 hours at 5MW. The total neutron flux was monitored by 3gr hornblende age standard [4], irradiated in the same sample holder. In the same batch, $CaSi_2$ and $KAlSi_3O_8$ salts were used for interfering isotope correction. A typical J-value was (1.729 ± 0.022) $\times 10^{-2}$. In stepwise heating experiment, the minerals were heated under defocused laser beam, and temperature of sub-millimeter grains was measured using infrared thermometer of which spatial resolution is 0.3 mm in diameter with a precision of 5 degrees. A feedback circuit for relatively long time-lag heating control is used not to overshoot the programmed temperature [5]. Argon isotopes were measured using a mass spectrometer with mass resolution of approximately 400, allowing to separate hydrocarbon from ^{39}Ar and other argon isotopes.

RESULTS: An example of ^{40}Ar/^{39}Ar age spectra of hornblende grains is illustrated in Fig. 1. The plateau age 1.965 Ga is consistent with 1.935 Ga of the biotite and the U-Pb age of apatite of the Acasta gneiss, These ages of ca. 1.9 Ga were obtained from samples approx. 20 km apart. Thus, it represents the cooling age of the regional metamorphism by Wopmay orogen. . SHRIMP U-Pb age study on zircon gave 4.0 Ga. The closure temperature (T_c) of zircon, 800 - 900 ^{o}C suggests that the Wopmay orogen heated the area above hornblende T_c, 500 ^{o}C, but
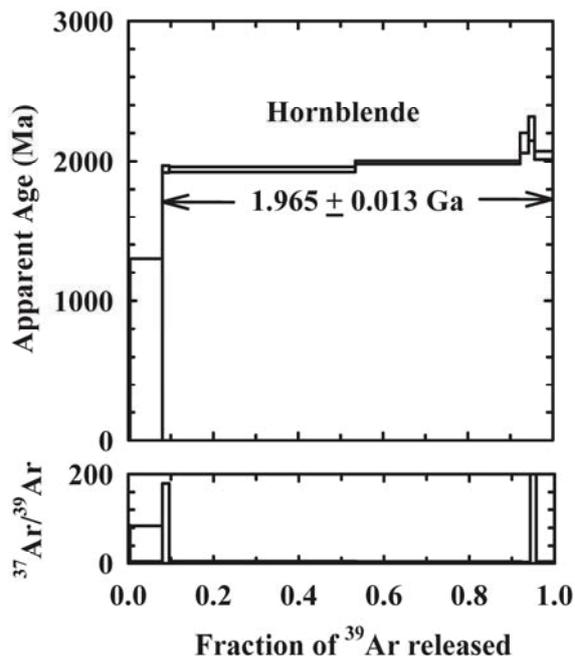

Fig. 1. ^{40}Ar/^{39}Ar age spectra of a hornblende grain from Acasta gneiss. More than 90% of total fraction defines plateau age of 1.965 Ga. The ^{37}Ar/^{39}Ar error (lower figure) seems to have little effect on the age in the plateau region.

not above zircon's T_c. The relatively small difference in the cooling ages between biotite and hornblende also suggests that the regional event has characteristics of a slow cooling process. A trial run on impurities in Acasta zircons was attempted. Because of its small amount and heat resistivity of zircon, we have not obtained conclusive results yet. A fraction with a small error gave an age ca. 2.0 Ga, suggesting age resetting of impurities in the zircons while U-Pb system is not.

REFERENCES:
[1] H. Hyodo, K.Sato, H.Kumagai and K. Takamiya, *KURNS Progress Report* 2019 CO5-7.
[2] S.A.Bowring and I.S. Williams, *Contributions to Mineralogy and Petrology*, **134** (1999) 3–16.
[3] Y. Sano, et al. *Geochimica Cosmochimica Acta* **63** (1999) 899–905.
[4] J.C. Roddick, *Geochim. Cosmochim. Acta* **47** (1983) 887-898.
[5] H. Hyodo, *Gondwana Research* **14** (2008) 609-616.

R2143